

International Journal of Modern Physics: Conference Series  
 © World Scientific Publishing Company

## The Need For Hard Spectra Sources of Nearby Heavy Cosmic Rays

Andrew M. Taylor \*

*Dublin Institute for Advanced Study, 31 Fitzwilliam Place,  
 Dublin 2, Ireland  
 taylora@cp.dias.ie*

Using recent Pierre Auger Observatory energy spectrum and composition analysis results, an investigation is carried out into the requirements placed on the UHECR sources. The spatial distribution of these sources is investigated along with the energy distribution of UHECR they output. These investigations reveal the need for local UHECR sources which output a hard spectrum of intermediate/heavy UHECR. These results demand that local (<80 Mpc) UHECR sources exist, placing exciting and difficult requirements on the local extragalactic candidate sources. From these results, a relation between the maximum energy ( $E_{\max}$ ) and the source spectral index  $\alpha$  is also noted, which results directly from the nature of the photo-disintegration losses.

*Keywords:* Keyword1; keyword2; keyword3.

PACS numbers: 95.85.Ry, 96.50.sb

### 1. Introduction

The origin of UHECR has been a long sought for aim of cosmic ray studies. Despite the considerable time that has passed since their discovery, the sources of these high energy particles remain unclear. The ‘‘Hillas criterion’’<sup>1</sup> for a candidate sources demands that  $E_{\max} = \beta_s R_s Z e B_s$ , where  $E_{\max}$  is the maximum energy particle that may be accelerated by a source of size  $R_s$  containing magnetic fields of strength  $B_s$  and an isotropic distribution of internal scatters moving at velocity  $\beta_s c$ . Applied to  $10^{20}$  eV nuclei, the  $R_s B_s$  parameter space quickly reduces viable sources to just a few potential candidates, whose scatters must be moving at velocities close to  $c$ . This constraint may be written as

$$\beta_s Z \left( \frac{R_s}{\text{kpc}} \right) \left( \frac{B_s}{0.1 \text{ mG}} \right) > 1 \quad (1)$$

Such considerations for source requirements present necessary but not sufficient conditions for an object to be considered a viable candidate UHECR source. On top of these demands, the radiative loss rates as well as the acceleration rates available within the sources must be taken into account. The maximal acceleration timescale, assuming this occurs at the Bohm limit, is  $t_{\text{acc.}} = E/(ZecB_s\beta_s^2)$ .

\*permanent address

Similarly, the synchrotron loss time is  $t_{\text{loss}}^{\text{sync.}} = \frac{9}{(8\pi Z^2 \alpha)} \frac{h}{E} \left(\frac{B_{\text{crit.}}}{B_s}\right)^2$ , where  $B_{\text{crit}} = 1.5 \times 10^{20}$  G. Thus, if the acceleration time equals the synchrotron loss time,  $E_{\text{max}} = \frac{9}{Z} \frac{hcB_s}{8\pi\alpha} \beta_s^2 \left(\frac{B_{\text{crit.}}}{Z\epsilon B_s}\right)^2$ . This places an extra constraint on the velocity of the scatterers present within the accelerator. Applied once again to sources of  $10^{20}$  eV nuclei,

$$\left(\frac{\beta}{Z}\right)^2 \left(\frac{30 \text{ mG}}{B_s}\right) > 1 \quad (2)$$

Finally, losses through pion-production/photo-disintegration interactions, which dominate energy losses for UHECR protons and nuclei, respectively, also place constraints on the source parameters. Approximating the loss time to  $\sim$ Myr, valid for energies above  $10^{20}$  eV, a final constraint on the source parameters is

$$Z\beta_s^2 \left(\frac{B_s}{0.1 \text{ mG}}\right) > 1 \quad (3)$$

The above results indicate that few candidate objects are able to satisfy the difficult constraints on the acceleration environment, with  $\sim$ mG magnetic fields and quasi-relativistic scatterers needed to be present in the acceleration environment. Furthermore, these constraints should be considered conservative since they neglect the fact that UHECR must also survive the extragalactic environment during their propagation from source to Earth. We here investigate this second aspect of the problem in order to determine constraints on the source distribution from these propagation constraints.

Recent measurements from the Pierre Auger Observatory (PAO) have revealed new information both on the cosmic ray spectral shape as well as the arriving composition. Of particular importance for this study are the composition sensitive parameter  $\langle X_{\text{max}} \rangle$  and  $\text{RMS}(X_{\text{max}})$ , which describe the first and second moments of the air shower distribution function. The PAO have released measurements of these two parameters for energies  $10^{18.5}$ – $10^{19.6}$  eV <sup>2,3</sup>. As shown in fig. 1, both the  $\langle X_{\text{max}} \rangle$  and  $\text{RMS}(X_{\text{max}})$  measurements by the PAO indicate that the composition starts to become heavier at high energies above  $10^{18.5}$  eV. On these plots, the different coloured bands indicate the theoretical predictions of the expected  $\langle X_{\text{max}} \rangle$  and  $\text{RMS}(X_{\text{max}})$  values for different (single composition) nuclear species. The width of these bands are provided to convey the present uncertainty which exists in the hadronic models used to calculate both the  $\langle X_{\text{max}} \rangle$  and  $\text{RMS}(X_{\text{max}})$  values. Interestingly, the use of the spread in this way has recently been bolstered by studies following the first LHC results <sup>4</sup>. Furthermore, as is also seen from the relative widths of these lines, of the  $\langle X_{\text{max}} \rangle$  and  $\text{RMS}(X_{\text{max}})$  model measurements, the relative uncertainty associated with the  $\text{RMS}(X_{\text{max}})$  for different species is smaller than that for  $\langle X_{\text{max}} \rangle$ .

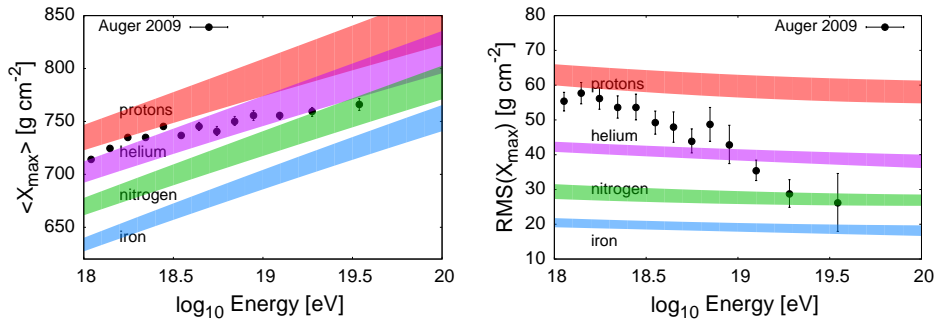


Fig. 1. Plots showing PAO measurements of the composition sensitive quantities  $\langle X_{\max} \rangle$  and  $\text{RMS}(X_{\max})$ .

## 2. Propagation Physics and Description

Before their arrival, UHECR must propagate across astronomical distances between their source and Earth. The arriving flux from an ensemble of their sources is naturally expected to contain a suppression feature just below the highest energies currently observed. Such a feature results as a consequence of UHECR interactions with background photons. For the case of a proton dominated UHECR composition, photo-pion production interactions will rapidly start to dominate energy losses at energies just below  $10^{20}$  eV, leading to a suppression feature being expected at these energies, referred to as the *Greisen-Zatsepin-Kuz'min* (GZK) cutoff<sup>5,6</sup>.

The expectation of a high energy suppression feature, however, is not unique to the proton composition scenario. Indeed a similar feature is also naturally expected for the case when a significant fraction of the population consists of nuclei. However, for such a scenario, it is instead photo-disintegration interactions which lead to the suppression in flux at the highest energies. Subsequently, the identification of a suppression feature at the highest energies is unable to provide much clue as to the underlying source composition.

In order to get a more developed understanding to allow the composition measurement results to be interpreted, the energy loss lengths for different species of UHECR nuclei must be calculated. The calculation of these loss rates follow the general formula,

$$R_{A,\gamma} = \frac{1}{2\Gamma_A^2} \int_0^\infty \frac{1}{\epsilon_\gamma^2} \frac{dn_\gamma}{d\epsilon_\gamma} d\epsilon_\gamma \int_0^{2\Gamma_A \epsilon_\gamma} \epsilon'_\gamma \sigma_{A\gamma}(\epsilon'_\gamma) K_{A\gamma} d\epsilon'_\gamma \quad (4)$$

where  $dn_\gamma/d\epsilon_\gamma$  describes the spectral shape of the target photons being interacted with,  $\sigma_{A\gamma}$  dictates the interaction rate of the UHECR with these target photons, and  $K_{A\gamma}$  is the fractional energy loss of the UHECR as a result of the interaction. Example energy loss rate curves for different species are given in reference<sup>7</sup>.

Using a complete set of such loss/interaction rate curves for the ensemble of nuclear species, the transmutation of species as they propagate through extragalactic

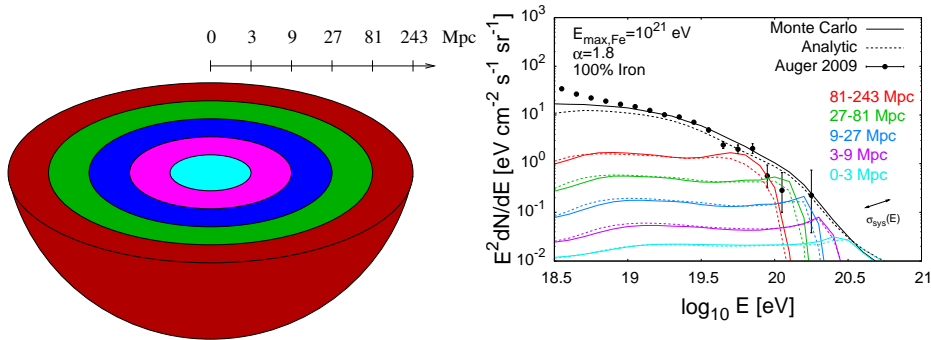


Fig. 2. Left-panel: a depiction of the source shells considered. Right panel: a spectral plot showing PAO measurements, Monte Carlo and analytic derived fluxes arriving from the different source shells.

radiation fields can be calculated. A Monte Carlo implementation for calculating the temporal evolution of the nuclear state populations was employed in reference <sup>7</sup>. For these calculations, all possible decay routes through a whole network of possible alternative nuclear isotope states were considered.

### 3. Results

In order to keep the situation of the UHECR propagation as simple as possible, the presence of extragalactic magnetic fields on UHECR propagation are neglected. Furthermore, with no prior knowledge about the UHECR source population, a “universal” (homogeneous and isotropic) distribution is generally assumed. We adopt this assumption here as a means of investigating signatures of a departure from it. In order to quantify the effect of a different source distribution in this paper, we separate out the fluxes produced from source regions with shells of radii 0-3 Mpc, 3-9 Mpc, 9-27 Mpc, 27-81 Mpc, and 81-243 Mpc surrounding the Earth, as depicted in the left-panel of fig. 2. In this way, the results obtained may be used to encapsulate the effects introduced by a non-“universal” local void of UHECR sources.

As was found in previous work<sup>8,9</sup>, the contour plots reveal that sources emitting intermediate-heavy compositions ( $A > 20$ ) UHECR with hard spectral indices ( $\alpha \lesssim 2$ ) and intermediate energy cutoffs ( $E_{\text{Fe,max}} \sim 10^{21}$  eV) are best able to describe the current data. It should also be noted that for light-nuclei type sources the contour space was found to be considerably diminished, with no good-fit contours existing for a proton-only scenario, even at the 99% C.L.

Interestingly, the introduction of a minimum distance to the first source can dramatically alter the good-fit contour plots, as shown in fig. 3. In particular, for the shell sizes considered, it is seen that for source emitting either silicon or iron type nuclei compositions, the 99% C.L. contours undergo a rapid decrease in size for minimum source distances in the range 9 – 27 Mpc and 27 – 81 Mpc respectively. Furthermore, these plots also indicate that for minimum source distances beyond

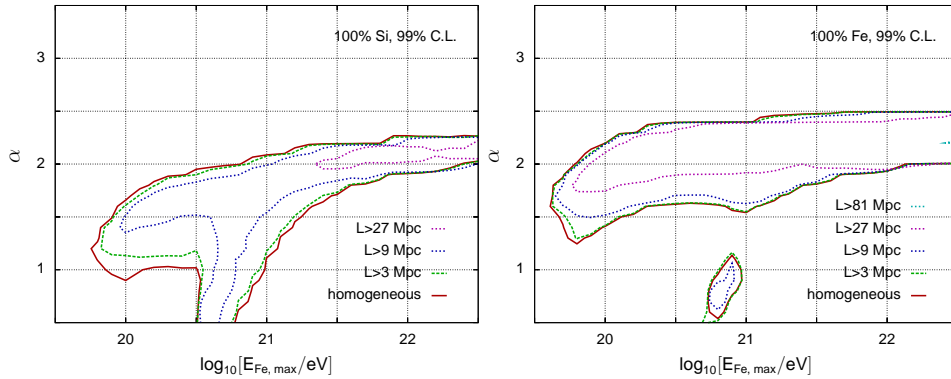


Fig. 3. The effect on the 99% C.L. silicon and iron contour plots by the introduction of a minimum source distance.

these constrained ranges, uncomfortably large cutoff energies,  $E_{\text{Fe,max}}$ , are required by the source population. This result encapsulates one of the key findings from this study, that **sources of hard spectra UHECR nuclei sources with local distances,  $\sim 40 - 80$  Mpc must exist in local extragalactic space.**

### 3.1. $E_{\text{min}}-\alpha$ Relation

Also noticed from the plots in fig. 3 is a general trend between the parameters  $E_{\text{max}}$  and  $\alpha$ , with larger cutoff energies ( $E_{\text{max}}$ ) allowing larger (softer) source spectral indices ( $\alpha$ ). The origin of this trend may be understood through a consideration of the propagated fluxes, for two differing cutoff energy cases, shown in the energy flux representation. The resulting fluxes for both a low ( $10^{20}$  eV) and medium ( $10^{20.5}$  eV) maximum energy cases for hard (1.2) and soft (1.8) source spectral indices are shown in fig. 4. Also shown in these figures are the source injection spectrum, which would have been the arriving flux spectrum for the case in which the particle energy loss processes are turned off.

For these calculations energy flux is largely a conserved quantity, with pair losses only mildly perturbing the overall arriving flux<sup>10</sup>. As a result of this approximate conservation law, the propagated fluxes for cases in which comparative values for the total injected energy flux is injected into the UHECR by the sources, result in comparable propagated fluxes. For these cases, photo-disintegration losses re-process the injected spectrum, resulting in a flattened (in the energy flux representation) arriving form for the arriving flux.

Following this investigation for a simplified single-composition model, it is also worthwhile checking that the general feature of the  $E_{\text{max}}-\alpha$  relation is preserved when more complicated admixtures of nuclear species are considered. Through the employment of the 3-component (protons, nitrogen, iron) composition model, the relation is indeed found to be preserved. Furthermore, the best-fit cases for such admixture scenarios indicate that the low ( $10^{20}$  eV) cutoff and hard (1.2) source

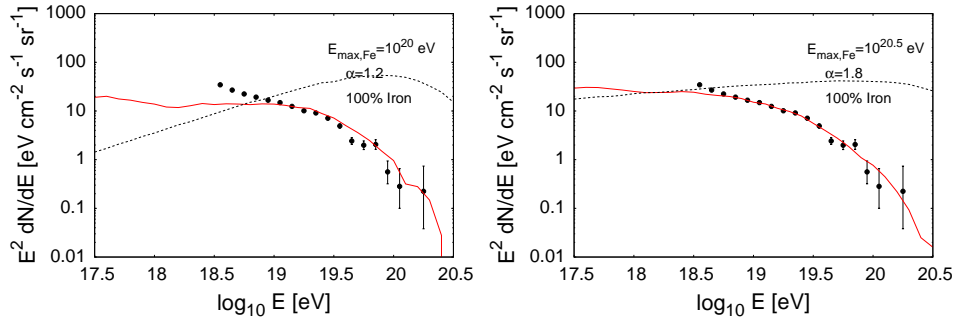


Fig. 4. A comparison of the propagated fluxes for an Iron only source composition. The left (right) panel shows the arriving energy flux for sources with maximum energy  $E_{\max} = 10^{20}$  eV ( $E_{\max} = 10^{20.5}$  eV) and spectral index  $\alpha = 1.2$  ( $\alpha = 1.8$ ).

spectrum case prefers a lighter admixture than the medium ( $10^{20.5}$  eV) and soft (1.8) source spectrum case.

#### 4. Conclusion

The increasing presence of nuclei in the UHECR arriving to Earth at high energies provides useful new information about the proximity and spectra of their sources. Investigations considering single composition source scenarios indicate that the spectral and composition results measured by the PAO place requirements on the source proximity and emission spectra. Specifically, the need for **local sources to exist which produce UHECR with a hard source spectra** is emphasised. Furthermore, a general relation on the maximum energy and source spectral index  $E_{\max} - \alpha$  is also noted from these results. Such requirements on the accelerator sites remain when the more general case of a mixed composition model for the sources are considered

#### Acknowledgments

A.T. acknowledges a Schrödinger fellowship at DIAS.

#### References

1. A. M. Hillas, *Ann. Rev. Astron. Astrophys.* **22**, 425 (1984).
2. M. Unger, f. t. P. A. Collaboration, arXiv:1103.5857 [astro-ph.HE].
3. J. Abraham *et al.* [Pierre Auger Collaboration], *Phys. Rev. Lett.* **104**, 091101 (2010).
4. D. d’Enterra, R. Engel, T. Pierog, S. Ostapchenko and K. Werner, *Astropart. Phys.* **35** (2011) 98 [arXiv:1101.5596 [astro-ph.HE]].
5. K. Greisen, *Phys. Rev. Lett.* **16**, 748 (1966).
6. G. T. Zatsepin and V. A. Kuz’min, *JETP Lett.* **4**, 78 (1966).
7. D. Hooper, S. Sarkar and A. M. Taylor, *Astropart. Phys.* **27** 199 (2007) [astro-ph/0608085].

8. D. Hooper and A. M. Taylor, *Astropart. Phys.* **33**, 151 (2010).
9. A. M. Taylor, M. Ahlers and F. A. Aharonian, *Phys. Rev. D* **84** (2011) 105007 [arXiv:1107.2055 [astro-ph.HE]].
10. M. Ahlers and A. M. Taylor, *Phys. Rev. D* **82** (2010) 123005 [arXiv:1010.3019 [astro-ph.HE]].